

# PERFORMANCE OF SINUSOIDAL P.W.M. CONVERTER FED D.C. MOTOR

BY

S. S. SHOKRALLA , S. A. MAHMOUD AND H. MEKHAHEEL  
FACULTY OF ENGINEERING , MENOUEFIYA UNIVERSITY  
SHBIN EL - KOM , EGYPT .

## ABSTRACT

This paper presents a new approach for simulation of a sinusoidal pulse width modulated converter fed DC motor in the presence of feeder impedance . The proposed simulation is used to predict and describe the system behaviour in transient and steady-state conditions .The suggested modelling is applicable to any number of pulses per half cycle .The steady-state waveforms are analyzed using Fourier series . The total harmonic distortion of supply current and AC motor input voltage are obtained . Moreover , the effects of chopping - to - supply frequency ratio and the modulation index on the performance are investigated .The computed performance is verified experimentally .The results show that the suggested modelling and simulation are accurate and convenient to predict the performance characteristics for such a system .

## INTRODUCTION

The phase control scheme is commonly used in solid - state control of DC drives [1-2 ]. In spite of the simplicity of this control scheme , the main disadvantages associated with such converters are poor input power factor specially at larger phase angle delays , the considerable lower order harmonic current in the AC supply , and ripples in the motor current under certain operating conditions , the motor current may become discontinuous ;this mode influences the dynamic response of the motor drive system [ 3 ].

These disadvantages have been partially solved by using an inductor capacitor filter at the input supply side and smoothing reactor in series with the motor armature . In this method , it is found that the current is large and the frequency is low, thus, large sized filters are required . In addition, the use of

*MANUSCRIPT RECEIVED FROM DR: S.S. SHOKRALLA AT: 27/7/1996,  
ACCEPTED AT 25/8/1996, PP 51-71  
ENGINEERING RESEARCH BULLETIN, VOL, 19, NO. 3, 1996  
MENOUEFIYA UNIVERSITY, FACULTY OF ENGINEERING,  
SHEBINE EL-KOM, EGYPT. ISSN. 1110-1180*

filters causes variation of the output voltage and increase losses .Moreover , the power factor may decreases despite the improvement in the waveforms . Addition of smoothing reactors in the motor circuit is not desirable from the standpoints of economy , weight, efficiency and dynamic response [ 4 ] . Alternatively, several conversion schemes using natural and forced commutation have been developed to improve the performance of DC drive systems . Although thyristor forced-commutated schemes , employing pulse width modulation control technique , are proved to achieve substantial advantages over the conventional phase-controlled schemes .The later still have the advantages of design simplicity , operation ,reliability and lower cost [ 5 ] .

Recently , the use of self-commutated converters , employing controlled on / off power switches such as power transistor , MOSFET , IGBT and GTO is a challenge to thyristor schemes withen the available power ratings .These PWM converters can efficiently and economically be employed in low and medium power applications of DC drive systems.While maintaining the advantages of design simplicity and operation reliability of naturally commutated schemes , they may efficiently compete with expensive and less reliable force-commutated schemes [ 6 ] .

Reported studies of AC - to - DC PWM converters vary in complexity and accuracy [ 7 - 10 ] .While References [ 7 - 8 ] dealt with passive R - L load circuits . Steady-state numerical solutions and performance evaluation of DC drive systems have been reported in References [4 , 9].The concept of harmonic reduction using PWM control strategy has been investigated underthe assumption of a flat-topped load current in order to simplify the analysis [11] . Implementation and steady-state modelling of DC drive system with uniform and sinusoidal pulse width modulation control have been investigated in References [5-6] ,but transient performance of DC motor fed from single-phase sinusoidal pulse width modulated converter has not been considered.

This paper presents a new approach for modelling and simulation of a separately excited DC motor fed from a sinusoidal pulse width modulated single-phase converter taking the feeder impedance into consideration.The aim of the proposed modelling and simulation technique is to obtain starting - up and steady-state performance characteristics . This technique is applicable for any number of pulses per half cycle . The effect of chopping to supply frequency ratio in addition to the modulation index over the load and supply harmonic contents are investigated . The general performance characteristics are also presented .Simulation results

are reported and proved to be in good agreement with the relevant experimental results.

#### DESCRIPTION OF THE SYSTEM

A schematic diagram of the system is shown in Figure (1) . It consists of a separately excited DC motor fed from a sinusoidal pulse width modulated (SPWM) single-phase converter taking the feeder impedance into consideration. A diode bridge rectifier is employed and a power MOSFET , operating in the chopping mode , is used to vary the amplitude of the average motor terminal voltage for speed control purpose .

#### DRIVE CIRCUIT

The drive circuit is shown in Figure (2) . This circuit employs phase-locked loop (PLL) principle to generate the required chopping frequency ( $F_c$ ) and hence the required number of pulses per half cycle . The (PLL) consists of two integrated circuits "4046" and "4040" . The input signal to "4046" is the output of the operational amplifier (OP1) which is synchronized with the sinusoidal supply voltage through a low pass filter . The operational amplifier (OP2) is used as a comparator for two signals , one of them from (PLL) and the other from the rectified voltage . The output of operational amplifier (OP3) is fed to an open collector which consists of two integrated circuits "7402" and "7406". This circuit protects the MOSFET and ensures that there are no signals on the MOSFET gate when there is no control voltage . The output of the open collector is fed to the gate of the power MOSFET . The parameter values of the designed system are given in Appendix (1).

#### PRINCIPLE OF OPERATION

The simulation and experimental waveforms for the drive circuit and gate pulses are shown in Figure (3) . Generation of the driving signals is accomplished by comparing a rectified sinusoidal voltage of variable amplitude ( $V_m$ ) and frequency ( $2 F_s$ ) with a triangular voltage of amplitude ( $V_c$ ) and frequency ( $F_c$ ). The ratio between ( $V_m$ ) and ( $V_c$ ) is defined as the modulation index (M) and is given as follows :

$$M = V_m / V_c \quad (1)$$

The average output voltage is varied by changing  $V_m$  . As a result of the rectification stage , the waveform of load voltage and current are repetitive at a frequency ( $F_o$ ) , and equals to double the supply frequency ( $F_s$ ) . Assuming that the chopping

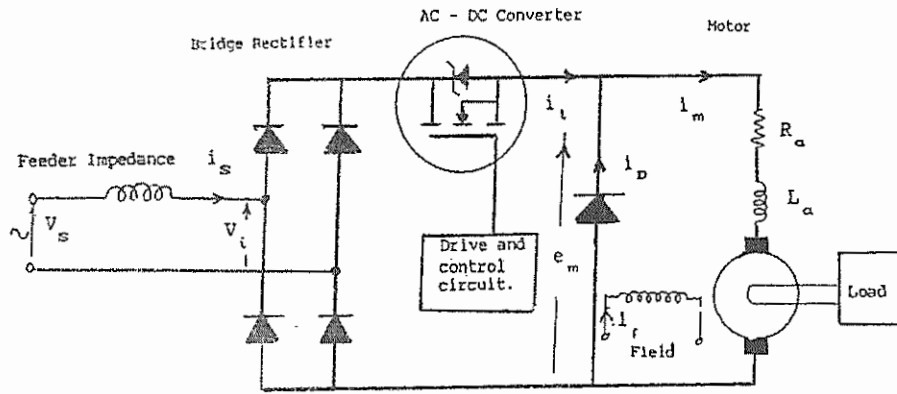


Figure (1) Schematic diagram of the system.

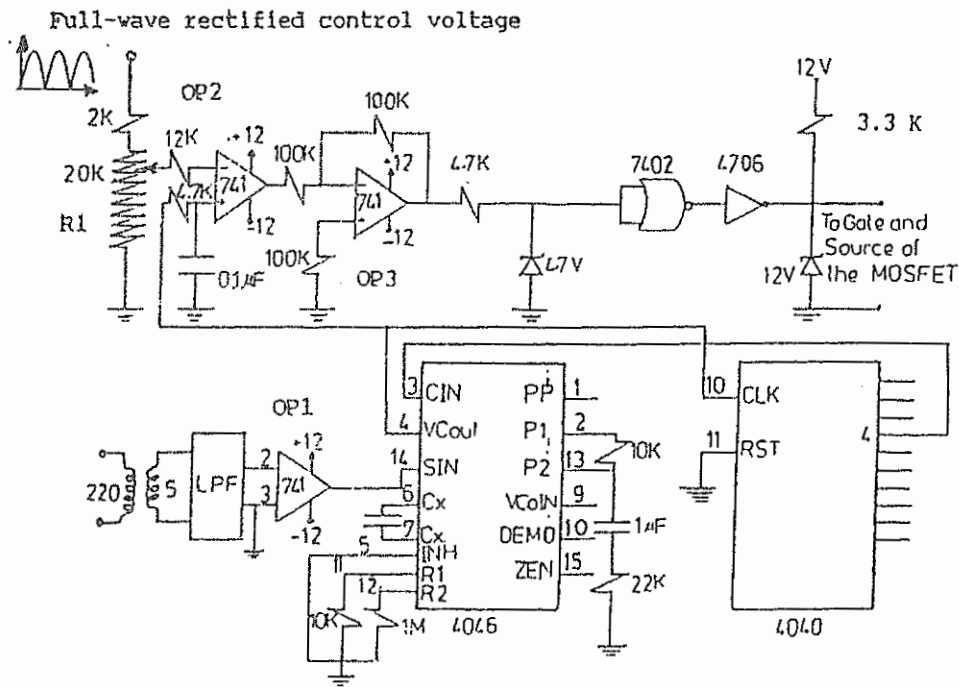
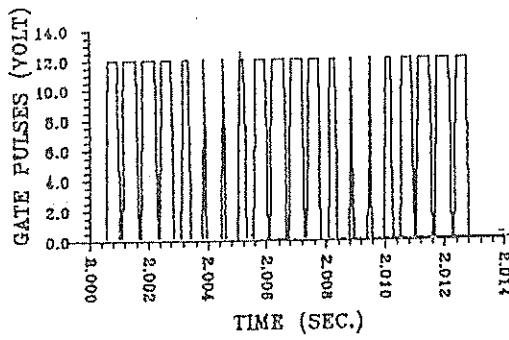
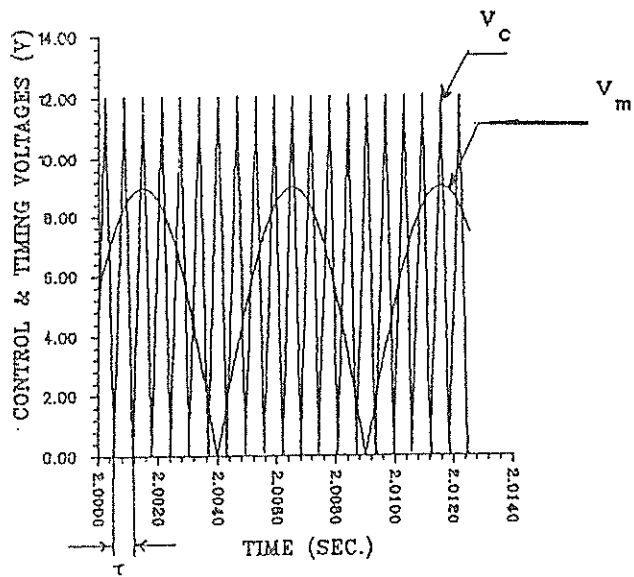
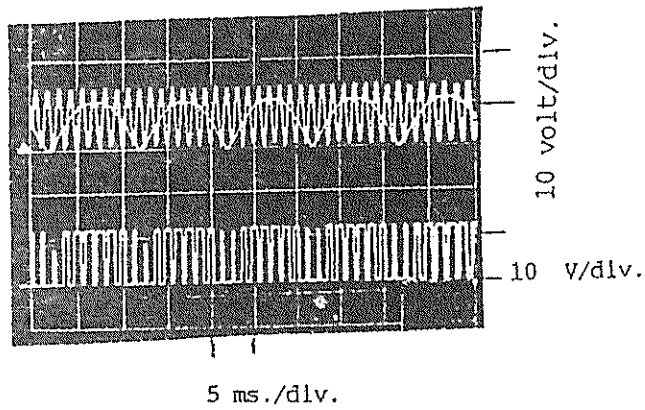


Figure (2) Drive and control circuit.



(a) Simulation waveform .



(b) Experimental waveform .

Figure (3) Simulation and experimental waveforms for drive circuit and gate pulses .

to supply frequency is given by  $\gamma$ , and providing that  $\gamma$  is a positive even integer, each half cycle of the sinusoidal supply contains  $NN$  chopping cycles is given by :

$$NN = \frac{\gamma}{2} = \frac{F_c}{2F_s} = \frac{F_c}{F_o} \quad (2)$$

The period of the chopping cycle is given by :

$$\tau = \pi / NN \quad (3)$$

The maximum average voltage corresponding to  $M = 1$ , depends on the amplitude of the supply voltage, which should be chosen for a given motor. Thus the maximum output voltage is given by :

$$V_{om} < \frac{2}{\pi} V_i \quad (4)$$

Where  $V_i$  is the peak of the sinusoidal motor input voltage. If the modulation index varies in the range  $0 < M < 1$ , the corresponding output average voltage varies in the range  $0 < V_o < V_{om}$ . It should be emphasis that  $V_{om}$  must be able to run the motor up to its rated loading conditions. This implies that  $V_{om}$  should be equal to the rated motor voltage.

#### MODELLING OF THE MOTOR

There are three modes of operation. The performance equations for each mode are expressed as follows:

##### MODE (1) Duty Interval :

This interval starts when the control voltage  $V_m$  is equal or greater than the triangular carrier wave  $V_c$ . This interval is terminated when  $V_c$  equals or exceeds  $V_m$ . The corresponding differential equations are as follows :

$$\frac{di_s}{dt} = \frac{1}{L_s} [V_s - V_i - R_s i_s] \quad (5)$$

$$\frac{di_m}{dt} = \frac{1}{L_a} [V_s - V_i - R_a i_m] \quad (6)$$

$$\frac{d\omega_m}{dt} = \frac{1}{J} [K_m i_m - F \omega_m - T_l] \quad (7)$$

##### MODE (2) Freewheeling Interval :

This interval starts when the power MOSFET is turned off and terminated when the diode current equals to

zero. The corresponding differential equations are as follows:

$$\frac{di_m}{dt} = \frac{1}{L_a} [ -K_m \omega_m - R_a i_m ] \quad (8)$$

$$\frac{d\omega_m}{dt} = \frac{1}{J} [ K_m i_m - F \omega_m - T_l ] \quad (9)$$

MODE (3) Coasting Interval :

This interval starts when the diode current equals zero and terminated when the control voltage equals the triangular carrier wave and the power MOSFET is turned on. The corresponding differential equations are as follows:

$$i_m = 0 \quad (10)$$

$$\frac{d\omega_m}{dt} = \frac{1}{J} [ -F \omega_m - T_l ] \quad (11)$$

#### MODELLING OF THE IMPULSE GENERATOR

From Figure (3) , the equation which represents the rectified modulating wave and the triangular carrier wave is given by the following expressions:

$$v_m = V_m | \sin(x) | \quad (12)$$

$$v_c = \left. \begin{aligned} & \frac{V_c}{\tau/2} x + V_c & 0 < \tau < \frac{\pi}{2NN} \\ & \frac{-V_c}{\tau/2} x + V_c & \frac{\pi}{2NN} < \tau < \frac{\pi}{NN} \end{aligned} \right\} \quad (13)$$

Where " X " is the instant in radians which changes from 0 to  $2\pi$  and the peak value of the control voltage " $V_c$ " equals 12 volt. The solution of these nonlinear differential equations is obtained numerically.

#### HARMONIC CALCULATIONS:

1- Harmonic Components of The Supply Current ( $i_s$ )

The harmonic component of ( $i_s$ ) is obtained using Fourier analysis , while the  $n$  th order harmonic component is given by :

$$i_{sn} = ( 1 / \sqrt{2} ) \sqrt{ a_n^2 + b_n^2 } \quad (14)$$

$$\phi_{sn} = \frac{1}{n} \tan^{-1} ( a_n / b_n ) \quad (15)$$

Where  $a_n$  and  $b_n$  are the Fourier coefficients.

The expressions for calculating the A.C. motor input voltage ( $v_i$ ) are similar.

## 2- Harmonic Distortion Factor of The Supply Current .

The total harmonic distortion factor is defined as the ratio of the total r.m.s. harmonic content to the fundamental component . The total harmonic components of the supply input current " $I_{SH}$ " is given by the following expressions:

$$I_{SH} = \sqrt{I_S^2 - I_{S1}^2} \quad (16)$$

Where  $I_S$  is the rms value of the the supply input current and  $I_{S1}$  is its fundamental component rms value.

$I_S$  is given by :

$$I_S = \left[ \frac{1}{2\pi} \int_0^{2\pi} i_S^2(\omega t) d(\omega t) \right]^{1/2} \quad (17)$$

The harmonic distortion factor of the supply current is given by :

$$THDF = I_{SH} / I_{S1} \quad (18)$$

Similarly, the expressions for calculating the AC motor input voltage ( $V_i$ ) take the same shape.

## 3-Power and Power Factor

The average power dissipated at the AC motor input voltage is given by :

$$P_{in} = \frac{1}{2\pi} \int_0^{2\pi} v_i(\omega t) i_S(\omega t) d(\omega t) \quad (19)$$

$$Pf_S = \frac{P_{in}}{v_i I_S} \quad (20)$$

## EFFECT OF PHASE SHIFT

It is proved that the phase shift (for lead and lag angles of both control and carrier voltages with respect to the supply voltage) gives the minimum total harmonic distortion in AC input current and highest supply power factor at zero phase shift as shown in figure (4).



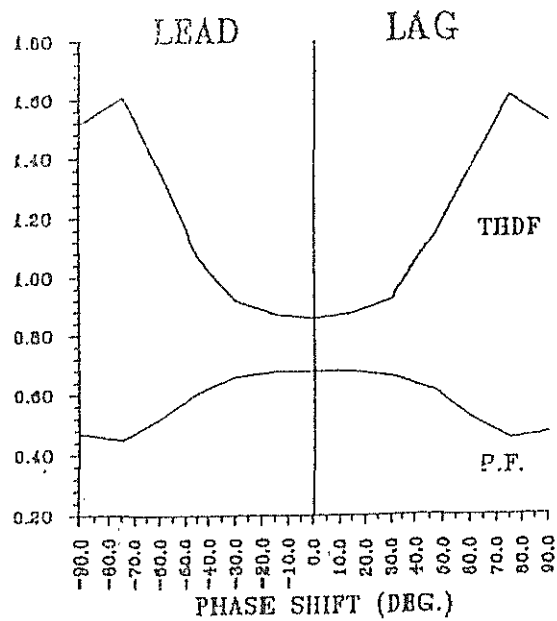


Figure ( 4 ) Effect of phase shift .

- (a) Supply current total harmonic distortion factor (THDF) .
- (b) Supply power factor (P.F.) .

### SIMULATION AND EXPERIMENTAL RESULTS

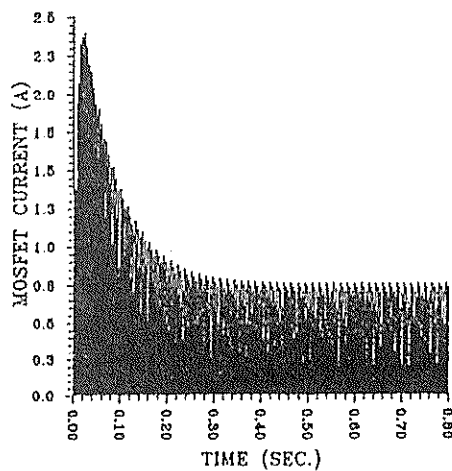
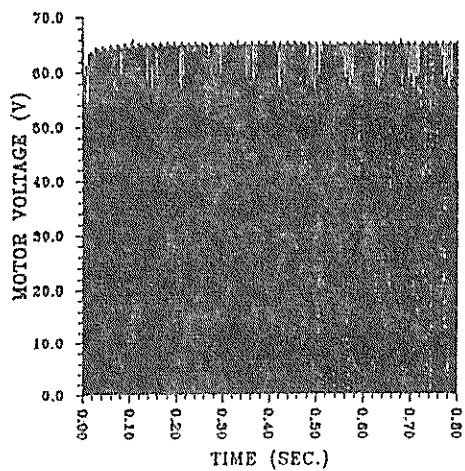
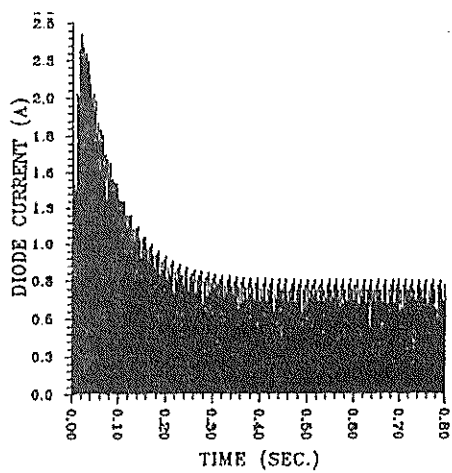
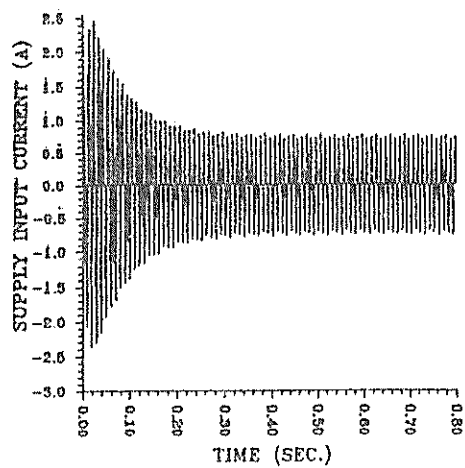
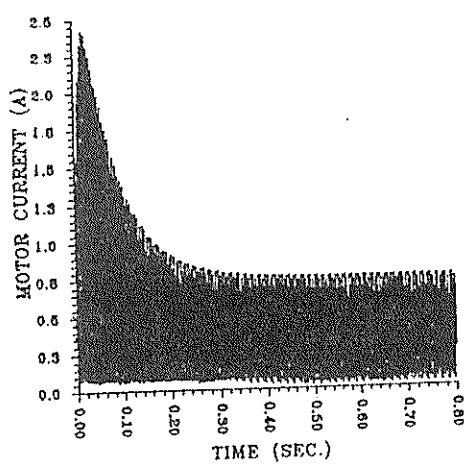
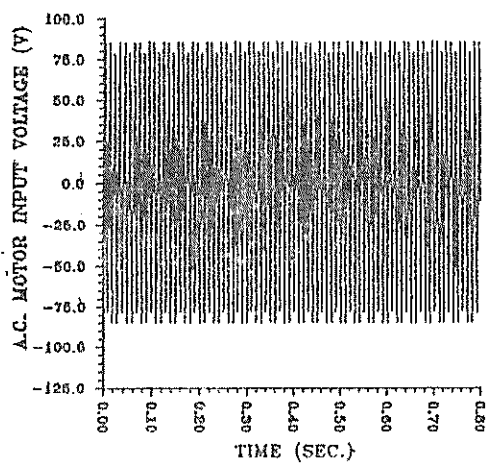
The system is implemented to verify the developed model. The behaviour of the proposed system under transient (starting-up) and steady-state conditions is determined by solving the foregoing nonlinear differential equations .The instantaneous and r.m.s. values of supply ,motor and diode currents , AC motor input voltage ,motor voltage ,developed torque and motor speed are obtained.

#### STARTING - UP AND STEADY-STATE PERFORMANCE

Figures (5,6) show the simulation and experimental waveforms for the starting - up performance of the motor . These results are taken with a chopping frequency of 800 Hz (8 pulses per supply half-cycle) , modulation index equals 0.8 and a load torque equals 1/3 full load .

Figures (7,8) show the above characteristics at steady-state condition .

The following performance characteristics are taken with a constant chopping frequency (NN = 8) at different values of modulation index ( M = 0.5 , 0.7 , 0.8 , 0.9 ) :



Simulation results

simulation results

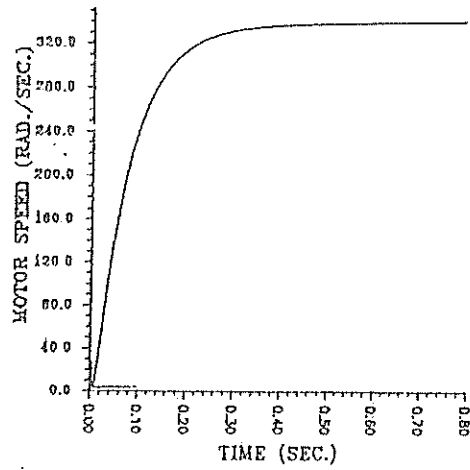


Figure ( 5 ) Simulation results during starting - up .

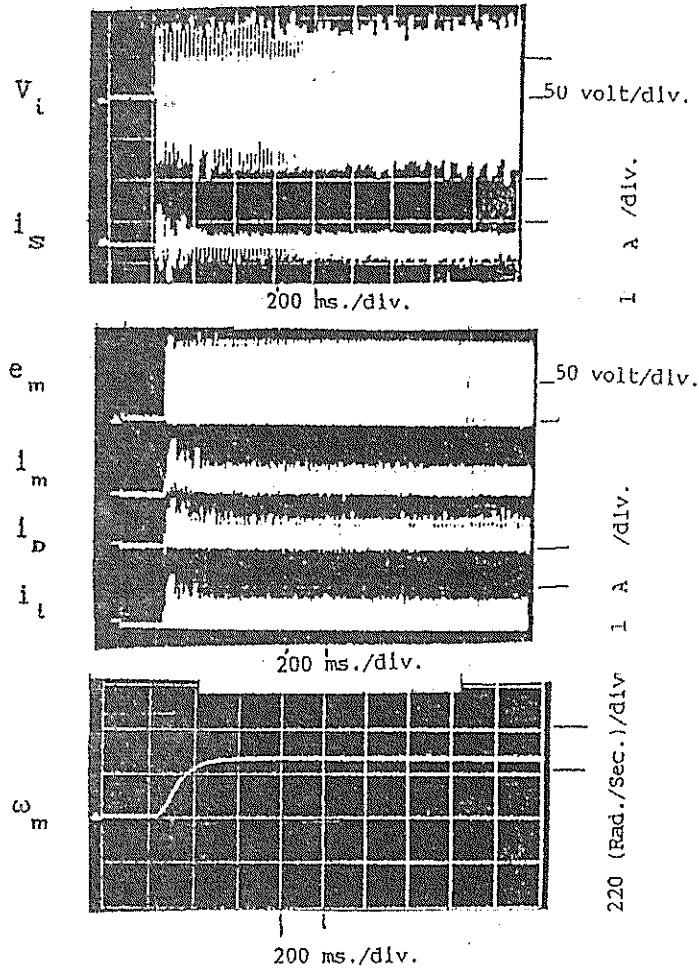


Figure ( 6 ) Experimental results during starting - up .

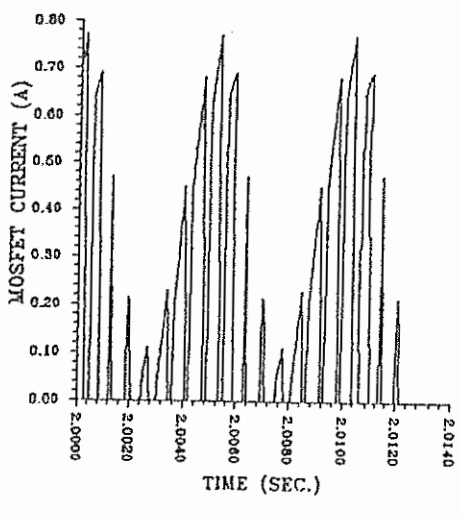
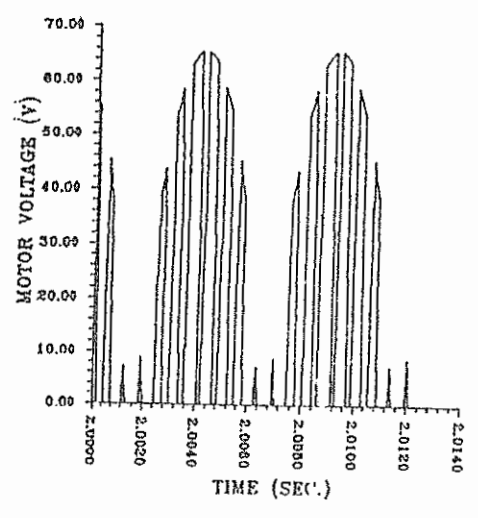
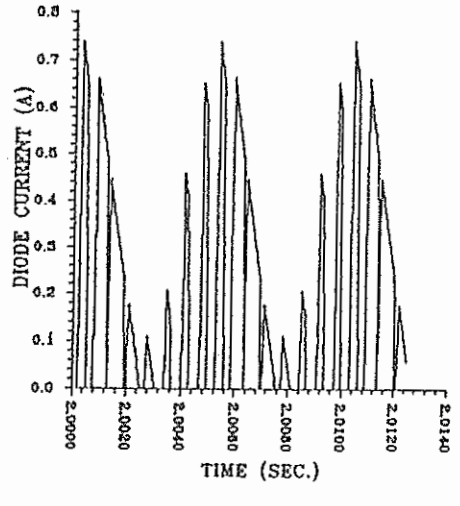
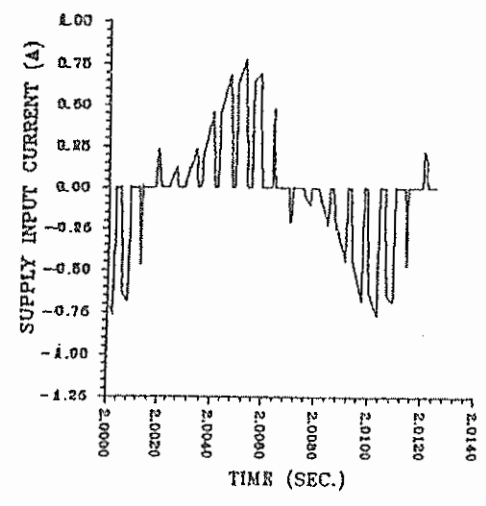
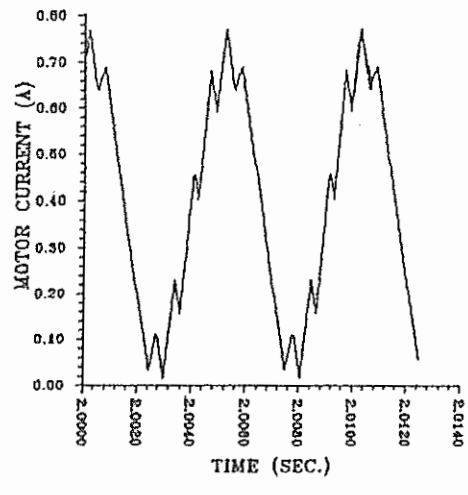
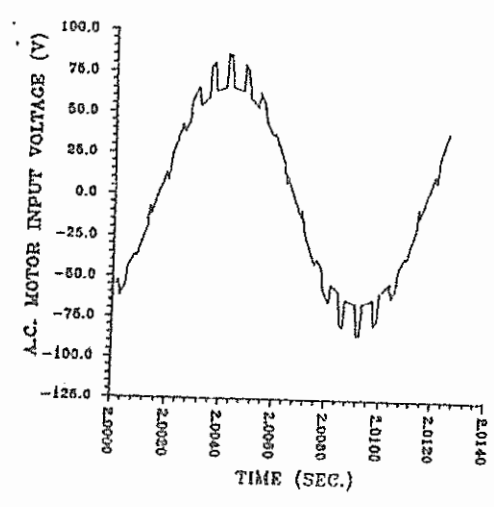
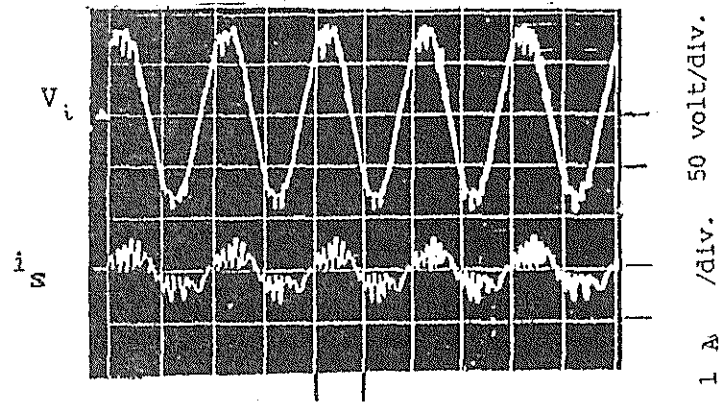
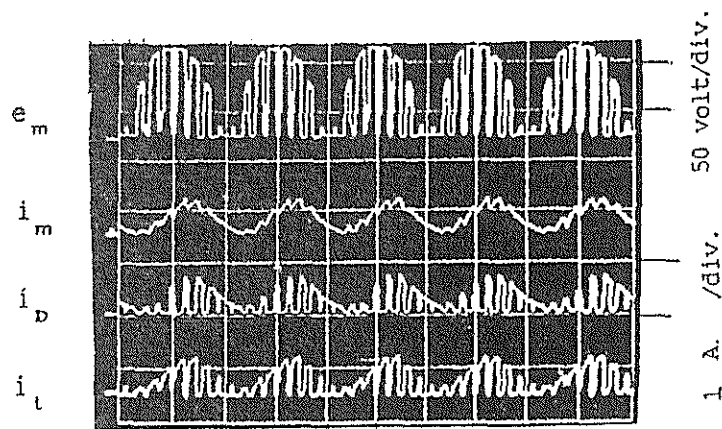


Figure ( 7 ) Simulation results at steady state .

Simulation results



10 ms./div.



5 ms./div.

Figure ( 8 ) Experimental results at steady - state .

Figure (9) shows the torque speed characteristics. It is observed that for different modulation indexes, speed regulation is good over most of operating range.

Figure (10) shows the variation of motor current ripple factor versus load torque. It is clear that the ripple factor decreases and hence the waveform improves with the increase of the modulation index (M).

Figures (11,12) show the variation of the total harmonic distortion factor for both the supply current and AC motor input voltage versus load torque. It is observed that the harmonic distortion factor decreases with the increase of the modulation index (M). This is because the MOSFET off periods are decreased.

Figure (13) shows the variation of supply input power factor versus load torque .It is observed that the

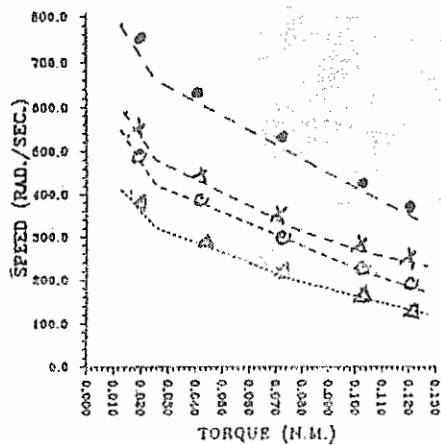


Figure ( 9 ) Torque speed characteristics .

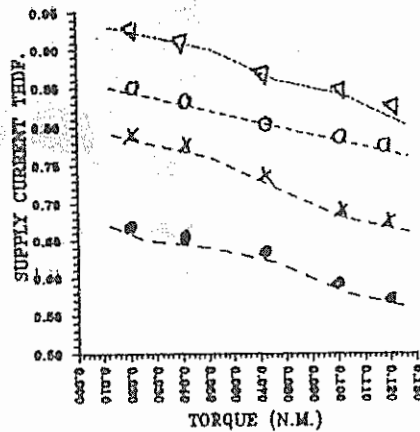


Figure (11) Supply input current total harmonic distortion factor (THDF) versus load torque

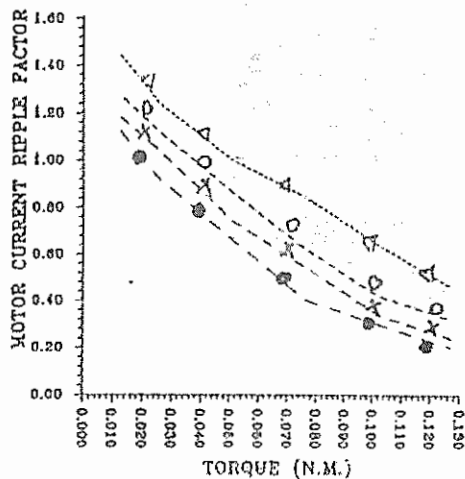


Figure ( 10 ) Motor current ripple factor versus load torque .

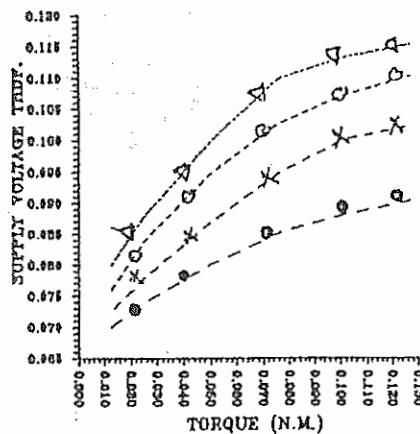


Figure (12) AC motor input voltage total harmonic distortion factor (THDF) versus load torque .

Computed results.



Experimental results.



Modulation index (M).

M = 0.5  
M = 0.6  
M = 0.8  
M = 0.9

With chopping frequency (NN) = 8

power factor increases with the increase of the modulation index(M).This may be attributed to the decreased total harmonic distortion factor of AC motor input voltage and current .

Figure (14) shows the variation of motor average voltage versus load torque .It is observed that with the increase of modulation index (M), the motor average voltage increases.

The following performance characteristics are taken with constant modulation index ( $M = 0.8$ ) at different values of chopping frequency ( $N = 5, 8, 16$ ).

Figure (15) shows the torque speed characteristics.It is noticed that the load torque decreases with the increase of the chopping frequency .This may be due to the decrease of the motor average voltage .

Figure (16) shows the variation of motor current ripple factor versus load torque.It is observed that the ripple factor decreases with the increase of the chopping frequency. This increase of the chopping frequency improves the chance of the system to operate in the continuous mode.

Figures (17,18) show the variation of the total harmonic distortion factor for both the supply current and AC motor input voltage versus load torque.It is found that the harmonic distortion factor increases with the increase of chopping frequency .This may be related to the increased MOSFET off periods .

Figure (19) shows the variation of supply input power factor versus load torque.It is observed that the power factor decreases with the increase of chopping frequency .This is because the total harmonic distortion of AC motor input voltage and current are increased.

Figure (20) shows the variation of motor average voltage versus load torque.It is clear that with the increase of chopping frequency , the motor average voltage increases.

#### CONCLUSIONS

The dynamic and steady-state characteristics of a sinusoidal pulse width modulated single-phase converter fed separately-excited DC motor drive , in the presence of feeder impedance , are predicted using the proposed modelling and simulation .This technique is applicable to any number of pulses per half-cycle . Moreover , the effect of modulating frequency on the motor characteristics and on the harmonic contents are demonstrated . The experimental and simulation results indicate that the developed model has a high accuracy

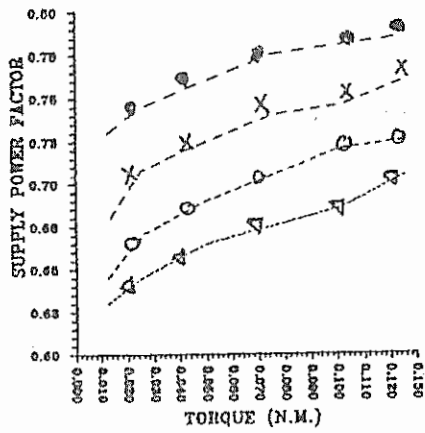


Figure ( 13 ) Supply input power factor versus load torque .

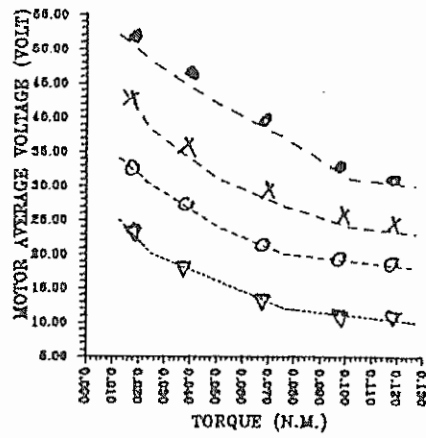
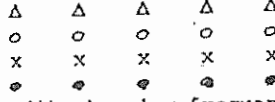


Figure ( 14 ) Motor average voltage versus load torque .

Computed results.



Experimental results.



Modulation Index (M).

- M = 0.5
- M = 0.6
- M = 0.8
- M = 0.9

With chopping frequency (NN) = 8

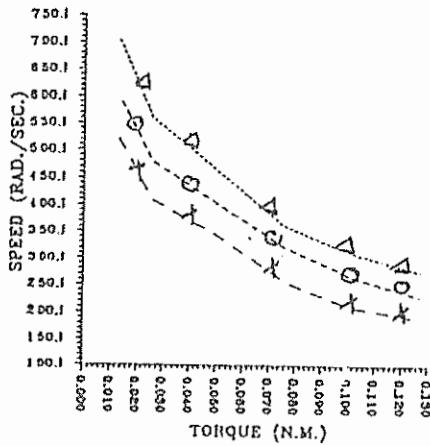


Figure ( 15 ) Torque speed characteristics

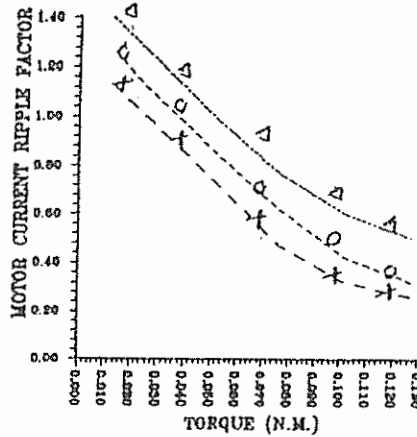
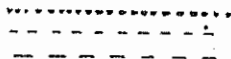
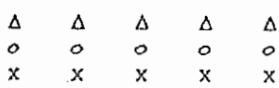


Figure ( 16 ) Motor current ripple factor versus load torque .

Computed results.



Experimental results.



Chopping frequency (NN)

- NN = 5
- NN = 8
- NN = 16

With modulation index (M) = 0.8



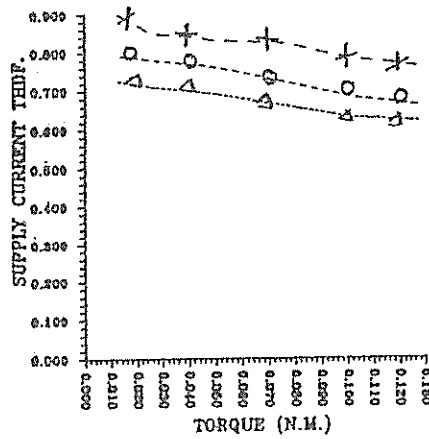


Figure (17) Supply input current total harmonic distortion factor (THDF) versus load torque

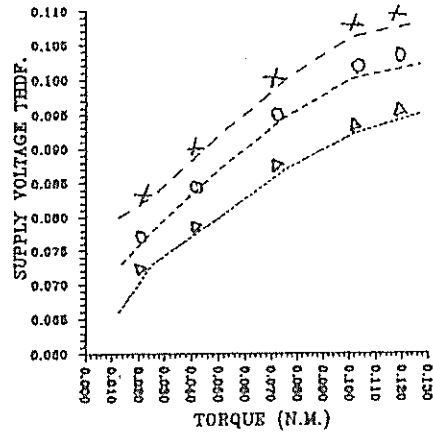


Figure (18) AC motor input voltage total harmonic distortion factor (THDF) versus load torque .

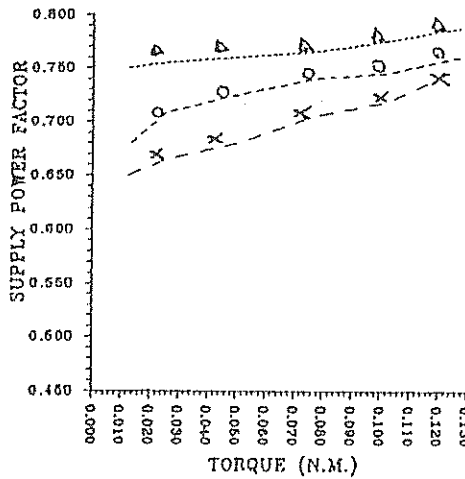


Figure (19) Supply input power factor versus load torque .

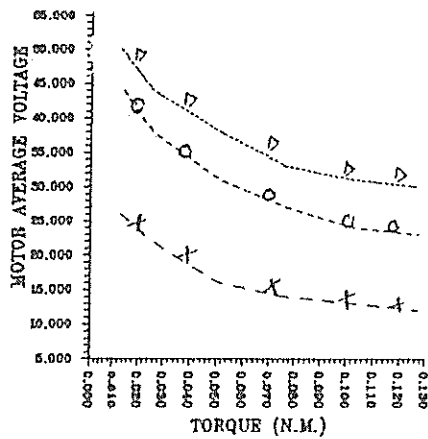


Figure (20) Motor average voltage versus load torque .

Computed results.

Experimental results.

Chopping frequency (NN)

.....  
 - - - - -  
 - - - - -

Δ Δ Δ Δ Δ  
 o o o o o  
 x x x x x

NN = 5  
 NN = 8  
 NN = 16

With modulation index (M) = 0.8

in predicting both starting-up and steady-state performance .The conclusions are summarized in the following points:

- The results reveal that the higher values of the chopping frequency improve the operation of the system.
- The chopping frequency affects the supply current harmonics . This leads to facilitate the filtration requirements of the supply current.
- It is found that the effect of chopping frequency on the ripple factor is noticed clearly at light loads .
- The total harmonic distortion factor decreases with the increase of modulating frequency , this is because the off periods of the power MOSFET are decreased.
- The power factor increases when modulating frequency is increased .This is because the total harmonic distortion factor decreases with the increasing of the modulating frequency.

#### REFERENCES

- [1] R.M. Dunaiski,"The effect of rectified power supply on large DC motors"AIEE Trans. part III(PAS) ,vol. 79, PP. 253 - 258 .June,1960.
- [2] Y. Onda ,S. Izawa ,and N. Kawakami,"Thyristor application to electric rolling stock",IEEE Trans. Ind. Gen. Appl. ,vol.IGA-5 ,Mar./April,1969.
- [3] K. G. Black ,"The effect of rectifier discontinuous current on motor performance",IEEE Trans. Ind.Appl.,vol.IA-83,1964.
- [4] Paresh C. Sen And S. R. Doradla,"Evaluation for control schemes for thyristor - controlled DC motors"IEEE Trans. on Industrial Electronics and Control Instrumentation ,vol.IECI - 25 ,no.3 ,PP. 247 -255,August,1978
- [5] S.A. Hamed and B.J. Chalmers,"Performance of variable-speed DC drive with sinusoidal PWM control"IEE, Sixth International Conference on Electrical machines And Drives, University of Oxford, UK,8 - 10 September ,1993.
- [6] S.A. Hamed "Steady-state modelling of a uniform pulse width modulated single phase AC -to- dc converter fed DC motor drive"ETEP vol.3 ,No.5 ,PP. 379-386,September /October ,1993.
- [7] S.Biswas , B.Basak and M.Swamy "A three-phase half-controlled rectifier with pulse width modulation"IEEE Trans. on Industrial Electronics ,38, PP. 121 -125 ,1991.
- [8] S. Biswas ,M. Mahesh and B. Lyenger "simple new PWM patterns for thyristor three-phase ac to dc converters"Proc.IEE,vol.133 ,PP. 354 - 358 ,1986.

[9] S. Doradla .C. Nagamani and S. Sanyai "A sinusoidal pulse-width modulated three-phase AC to DC converters fed DC motor drive" IEEE trans. on Industrial Applications ,21,PP.1394 - 1408 ,1985.

[10] T. Kataoka , K. Mizumachi and S. Miyairi "A Pulse width controlled AC to DC converter to improve power factor and waveform of AC line current"IEEE Trans.on Industry Applications, 15 ,PP. 670 - 675 .1979.

[11] K. Krishnamurthy ,G. Dubey and G. Revankar "converter control with selective reduction of line harmonics"Proc.IEE ,vol. 125 ,PP. 141 - 145 ,1978.

#### NOMENCLATURE

$e_m$	: Instantaneous motor voltage .
$F$	: Viscous friction coefficient (Nm/rad/sec.).
$F_s$	: Supply frequency.
$\gamma$	: Chopping to supply frequency ratio = $F_c / F_s$ .
NN	: Number of pulses per supply half-cycle = $\gamma/2$ .
$N_r$	: Motor speed (r.p.m.).
$i_D$	: Instantaneous diode current.
$i_m$	: Instantaneous armature current.
$i_t$	: Instantaneous MOSFET current.
J	: Moment of inertia ( $\text{Kg.m}^2$ ).
$K_m$	: Back e.m.f. coefficient [volt/(rad./sec)].
$R_a, L_a$	: Armature resistance and inductance.
$R_s, L_s$	: Feeder resistance and inductance.
$T_l$	: Load torque (N.m.).
$v_s, V_s$	: Instantaneous and peak values of supply voltage.
$v_i, V_i$	: Instantaneous and peak values of AC motor input voltage.
$v_m, V_m$	: Instantaneous and peak values of modulating wave.
$v_c, V_c$	: Instantaneous and peak values of carrier wave.
M	: Modulation index.
$\tau$	: Chopping period (Rad).
$\omega$	: Supply angular velocity (Rad./sec.).
$\omega_m$	: Motor angular velocity (Rad./sec.).

## APPENDIX

### (1) Motor parameters:

The test motor is a separately excited DC motor , 50 volt , 50 watt , 1 ampere , 3000 r.p.m. having the following measured parameters:

$R_a = 10.5 \text{ ohm}$  ,  $L_a = 0.06 \text{ henry}$  ,  $R_f = 550 \text{ ohm}$  ,  
 $F = 0.00001 \text{ volt}/(\text{rad}/\text{sec.})$  ,  $K_m = 0.127 \text{ N.m}/\text{rad}/\text{sec}$  ,  
 $J = 0.00012 \text{ Kg.m}^2$  ,  $V_s = 95 \text{ volt}$  ,  $V_i = 85 \text{ Volt}$  .

### (2) Supply feeder parameters :

$R_s = 1.5 \text{ ohm}$  ,  $L_s = 0.03 \text{ henry}$

## أداء محرك تيار مستمر مغذى بمغبر يعمل بالتعديل الجيبى لإتساع النبضات

### ملخص البحث

يقدم هذا البحث دراسة نظرية وعملية لدراسة أداء محرك تيار مستمر ذو تغذية منفصلة مغذى عن طريق مقوم يعمل بالتعديل الجيبى لإتساع النبضات. ويبين التمثيل العددي المقترح أداء هذا النظام فى حالة الاستقرار والحالات العابرة. ويتميز التمثيل المقترح بقابليته للتطبيق لأى عدد من النبضات فى خلال النصف دورة.

تم فى هذا البحث تحليل اشكال الموجات لكل من التيار والجهد المتغير الداخلى للمقوم وذلك للحصول على معامل التشوه الذى يؤثر على الأحمال الأخرى المتغذاه من نفس المصدر. وايضا تم دراسة تأثير زيادة تردد التقطيع بالنسبة لتردد المنبع وتأثير دليل التعديل على خواص النظام.

تم بناء النظام المقترح ووضحت النتائج العملية أن هناك تطابقا كبيرا بينها وبين النتائج التى تم الحصول عليها من التمثيل العددي. وأبرزت النتائج العملية والنظرية أن معامل القدرة عالى القيمة وأن التوافقيات ذات الترددات المنخفضة التى يكون ترشيحها صعبا يمكن الغاؤها أو تخفيضها بإختيار عدد النبضات لكل نصف دورة.